DEPARTMENT OF MECHANICAL ENGINEERING

Report on the Fracture Mechanics Testing of the Bond between Composite Overlays and Concrete Substrate

Victor Giurgiutiu[1], Dorothy Laub[2], Shannon Whitley[3]
Jed Lyons[1], and Michael Petrou[4]
University of South Carolina, College of Engineering,
300 S. Main St., Columbia, SC 29208
803-777-8018, FAX 803-777-0106, victorg@sc.edu

REPORT # USC-ME 98-101

COLLEGE OF ENGINEERING • UNIVERSITY OF SOUTH CAROLINA
COLUMBIA • SOUTH CAROLINA • 29208 • 803-777-4185

Report on the Fracture Mechanics Testing of the Bond between Composite Overlays and Concrete Substrate

Victor Giurgiutiu[1], Dorothy Laub[2], Shannon Whitley[3]
Jed Lyons[1], and Michael Petrou[4]
University of South Carolina, College of Engineering,
300 S. Main St., Columbia, SC 29208
803-777-8018, FAX 803-777-0106, victorg@sc.edu

REPORT # USC-ME 98-101

ABSTRACT

Strength, durability and health monitoring aspects of composite overlays on civil engineering structures are discussed. The perspective and benefits of the repair, upgrade, retrofit, and rehabilitation of US civil infrastructure using composite overlays is briefly reviewed. Bond strength, durability, and in-service health monitoring are identified as critical issues blocking the wide acceptance of these novel structural systems in the construction engineering community. A theoretical and experimental research program, set up at the University of South Carolina, is briefly presented. Specimen preparation, test schedules, modeling efforts, and proposed outcomes are discussed. The wider perspective of developing national standards and engineering guidelines for the design and utilization of composite overlays on civil infrastructures is also embraced.

---

[1] Associate Professor, Department of Mechanical Engineering
[2] Graduate Research Assistant, Department of Mechanical Engineering
[3] Undergraduate Research Assistant, Department of Mechanical Engineering, currently with Underwriters Laboratories, Rayleigh, NC.
[4] Assistant Professor, Department of Civil and Environmental Engineering

TABLE OF CONTENTS

1. INTRODUCTION

According to the US Department of Transportation and the Federal Highway Administration, there are about 576,000 bridges in the national bridge inventory, and 23% of these are structurally deficient or in need of repair. Several States have demonstrated that advanced fiber reinforced polymers (FRP) can be used to maintain and to improve the load capacity of concrete bridges. FRP repair technology offers a practical way to rehabilitate aging concrete bridges without disrupting traffic flow. In addition, masonry buildings form an important component of the US structural systems. Many of these have also historical value. Repair, rehabilitation and upgrade of masonry are required to meet new strength and seismic requirements. FRP composite overlays provide a viable solution to masonry maintenance. However, for both concrete and masonry applications, improvements are still needed in the resin systems to increase its adherence to summary prepared surfaces. Another major obstacle in the widespread use of these new engineering solutions is the lack of standards and practices for assessing the quality of the repairs and the durability of the composite-to-concrete bond. Figure 1 presents examples of composite overlay repairs of civil infrastructure — bridge columns, bridge decks, parking deck beams, etc. Quattrone, Berman and Kamphaus (1998) reported application of composite overlays to masonry upgrades. Laboratory tests with 4-ft by 4-ft masonry specimens were reinforced with a variety of composite systems: glass, Kevlar, or carbon fibers (unidirectional or woven) in epoxy, polyester or phenolic resins and tested to failure under shear loading. These preliminary tests revealed the bond between the composite overlay and the substrate, and not the basic strength of the composite, are the determinant factor for the ultimate strength. Further investigation of the fracture mechanics of the bond between polymeric composites and concrete substrates was performed in the College of Engineering of the University of South Carolina, as reported in the present document.

1.1. Composite Overlay Systems

Composite overlays are thin sheets of fiber reinforced polymeric material (1/8-in to 1/4-in) adhesively bonded to conventional construction engineering materials. Candidate polymeric systems include polyester, vinylester, epoxy and phenolic. Fibers can be glass, carbon, Kevlar, or combinations thereof. Glass and Kevlar fibers come in a variety of forms including weaves and non-woven fabrics. Carbon fibers can be woven, but common usage relies on unidirectional prepregs. The composite may be applied as: (a) wet lay-up; or (b) precured panels; or (c) partially cured prepregs. For wet lay-up and prepreg systems, the adhesive is the polymeric resin itself. For precured rigid panels, separate adhesive material needs to be used. Structural upgrades with composite overlays offer considerable advantages in terms of weight, volume, labor cost, specific strength, etc. However, one critical issue raised by the structural engineers is the still unknown in-service durability of these new material systems. Their ability to safely perform after prolonged exposure to service loads and environmental factors must be ascertained before wide acceptance in the construction engineering community is attained.

Figure 1 Composite overlay repair/upgrade of civil infrastructure: (a) circumferencial reinforcement of a bridge column; (b) bending reinforcement of a concrete deck; (c) shear reinforcement of a parking deck beam (*Composites Design and Applications,* Winter 1996 and January/February 1997).

Figure 2 presents a bridge placed on road S98 near Charleston, SC. The bridge has been experimentally strengthened with carbon-fiber composites through a joint effort between SC-DOT and Amoco Chemicals, Inc. This application is considered typical of the repair, rehabilitation, upgrade and strengthening to be performed on much of the nation's aging infrastructure. Though the performance of composite overlays is undoubtedly strong and long lasting, the connection between the concrete and the polymeric composite may present several durability problems. Disbonding of the composite overlay from the concrete substrate may have catastrophic results.

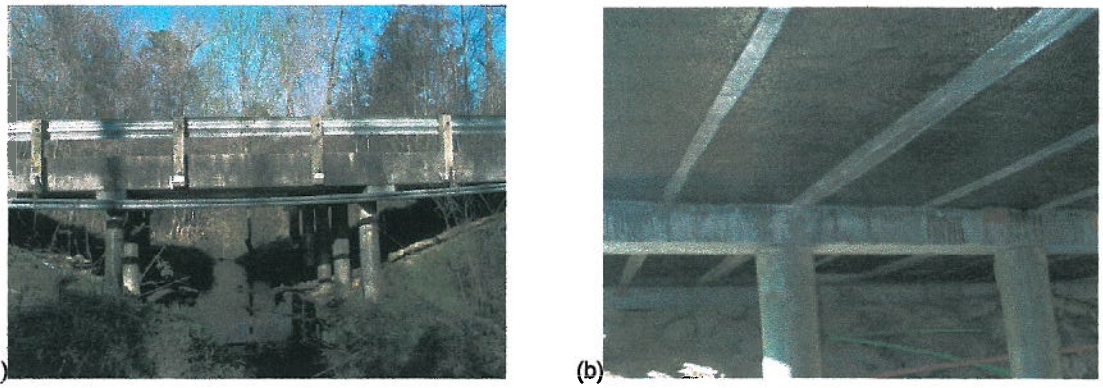

Figure 2 Full-scale verification of the research results to the health monitoring of civil engineer structures will be performed on this test-bed bridge placed on road S98 near Charleston, SC. The bridge has been experimentally strengthened with carbon-fiber composites through a joint effort between SC-DOT and Amoco Fibers, Inc.: (a) overall view of the bridge; (b) details of the columns and the underside of the bridge deck showing carbon fiber composites (photo: University of South Carolina, Mechanical Engineering Dept.).

1.2. Strength and Durability of Composite Overlaid Structures

Degradation or loss of performance of composite overlays on concrete or masonry may result from: (a) degradation of the composite overlay; (b) deterioration of the concrete/masonry substrate; and (c) loss of adhesion between the overlay and the substrate. Degradation of the composite and deterioration of the concrete/masonry substrates have been extensively researched elsewhere and will not be discussed here. Sufficient data exists to date to prevent early failure in composites, concrete, and masonry. However, the durability of the bond between the composite and the substrate remains a critical issue. Sudden loss of bond through wide area delamination – when it happens – can lead to catastrophic failure of the structure. Hence, loss of adhesion between the composite overlay and the substrate remains a critical factor. Maintenance of good adhesion between the composite overlay and the substrate structure is of paramount importance for assuring long-term performance and for preventing early failure of such structural upgrades and repairs. Though disbond prevention is critical, factual data it is not readily available. To date, this phenomenon has not been extensively studied and is insufficiently documented. In fact, little is known about the strength and durability of the bond between polymeric composites and conventional construction materials such as masonry and concrete.

The loss of adhesion and performance degradation can be traced to the interface between the composite overlay and the concrete/masonry substrate. The bond degradation manifests itself in the form of cracks, disbonds and delaminations. Cracks start at the outer limits and propagate towards the center. As cracks propagate, they generate disbonds and, eventually, large area delamination. Crack propagation is promoted by thermo-environ-mechanical cycling. Crack propagation can be delayed and even prevented by increasing the inherent fracture toughness at the composite/substrate interface. The intricate mechanism of crack propagation in an adhesive joint makes the subject of extensive research being carried out in academia, industry and government labs. At the University of South Carolina, a research program into the strength and durability of composite overlays on construction engineering materials has recently been initiated. Specimen preparation, test schedules, and modeling efforts are underway through a joint effort between the Mechanical and Civil Engineering Departments. In-situ health monitoring solutions and durability prediction codes are also studied. The long-term perspective of this program is to develop national standards and engineering guidelines for the design and utilization of composite overlays on civil infrastructures. The test schedule (Table 1) allows for the gradual transition from inexpensive coupon tests, to scaled structural components, up to the full-scale tests. In the present paper, attention is focused on the peel resistance and bond strength tests. These tests are performed on coupon specimens in order to assess the fracture mechanics behavior of the bond between the composite overlay and the concrete substrate. Data collected during these tests serves as baseline input for future tests to be performed on larger components and on full-size structures.

Table 1 Proposed test schedule for the evaluation of composite overlays on civil infrastructures.

	Test type	Specimen scale		
		Coupon specimens	Scaled structural components	Full-size civil infrastructures
1	Peel resistance and bond strength	X		
2	Crack resistance and fracture toughness	X		
3	Accelerated environmental exposure	X		
4	Structural strength increase via composite overlay		X	
5	Health monitoring methods	X	X	
6	Long-term environmental exposure			X

2. THEORETICAL BACKGROUND

The durability of the adhesion between the composite overlay and the concrete substrate is related to the initiation and propagation of cracks in the composite–concrete interface. For good durability, the composite-concrete material system should have high resistance to crack propagation, i.e. high fracture toughness. Crack initiation and propagation in the composite–concrete interface can be experimentally studied using the energy release rate method. In this approach, the energy released during crack advancement is determined using a compliance technique. This section briefly reviews the theoretical background involved in this approach, and develops the equations needed for processing and interpretation of test data. References are made to appropriate journal publications and ASTM standards.

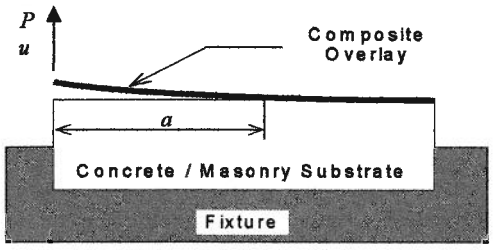

Figure 3 Schematic representation of a composite overlay being delaminated from a concrete/masonry substrate.

2.1. Energy release rate

Figure 3 presents a test specimen made up of a massive substrate and a composite overlay bonded on its top surface. Since the massive substrate is more rigid than the composite overlay, the deformation of the latter is much larger than of the former. Hence, the investigation can be confined to the study of the deformation and associate strain energy of the composite-layer. The composite layer is modeled as a simple beam of width b, thickness h, and elastic modulus E_{11}. Assume that, at a certain moment in time, the composite layer has delaminated, and a crack of length a is present in the interface between the composite and the substrate. To induce further delamination, the end of the composite is pulled upwards. As displacement u increases, so does the reaction force P. At a certain value of the P-u pair, the crack starts propagating, promoting further delamination. At this instance, the displacement, u, is kept constant (line AB in Figure 4). As the crack grows from a to $a + da$, the load decreases from P to $P - dP$. The strain energy released during this process is represented by the area OAB = $\frac{1}{2}udP$. This release of strain energy is used to promote crack advancement (creation of new material surfaces as the crack advances in the interface). The strain energy released during the advancement of a crack of unit length for a specimen of unit width is called *strain energy release rate* and is denoted by SERR or G. This quantity is also known as *crack-extension force*. Under fixed-grips conditions, the relationship between strain energy release rate, G, and the loading variables, P and u, is given by

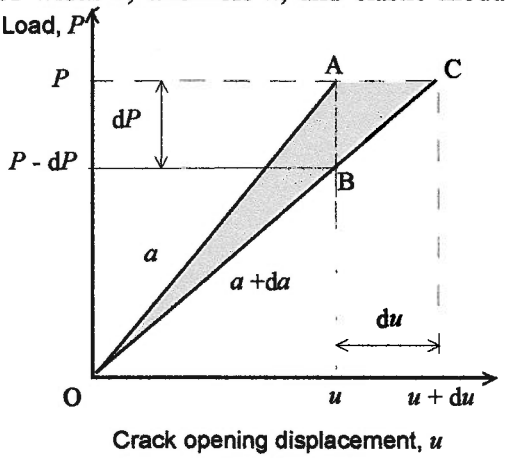

Figure 4 Load-displacement diagram

$$G = -\frac{1}{b}\frac{\frac{1}{2}u \cdot dP}{da}, \qquad \text{(fixed grips)} \qquad (1.)$$

where the negative sign signifies the fact that strain energy is being released.

2.2. Compliance-Formulation of Strain Energy Release Rate

One way to calculate the strain energy release rate, G, is *via* the compliance approach (Lubahn, 1959). The load-placement relationship can be written as

$$u = C(a)P, \tag{2.}$$

where $C(a)$ is the compliance value for a given crack length, a. Differentiating $u = C(a)P$ with respect to a, and using u = constant, i.e., $du = 0$, yields:

$$du = C(a)\cdot dP + P\cdot dC(a) = 0 \tag{3.}$$

Hence, multiplication by P, substitution of $P^2 = u^2/C^2$, and use of equation (1) yields

$$G = \frac{1}{2b}\frac{u^2}{C^2}\frac{\partial C}{\partial a} \qquad \text{(fixed-grips)} \tag{4.}$$

For convenience, Equation (4) can also be expressed in terms of the load, P, i.e.,

$$G = \frac{P^2}{2b}\frac{\partial C}{\partial a} \qquad \text{(fixed-grips)} \tag{5.}$$

2.3. Strain Energy Release Rate of a Debonding Composite Layer

The tip deflection of a simple beam of length a, width b, thickness h, and modulus E_{11} is

$$u = \frac{Pa^3}{3E_{11}I}, \qquad I = \frac{bh^3}{12}. \tag{6.}$$

Using equation (6), we express the compliance as

$$C(a) = \frac{a^3}{3E_{11}I}. \tag{7.}$$

Equation (7) indicates that the cubic root of compliance varies linearly with the crack length, a, i.e.,

$$C^{1/3} = m\cdot a, \qquad m = \left(\frac{1}{3E_{11}I}\right)^{1/3}. \tag{8.}$$

Differentiation of Equation (7) with respect to a, and use of Equation (8) yields the SERR expression:

$$G = \frac{3m^3a^2P^2}{2b} \tag{9.}$$

2.4. Relevant ASTM Standards

No standards could be found in the literature that specifically address the testing of the bond fracture toughness for composite overlays applied to concrete or masonry materials. However, standards describing related tests could be found. ASTM standard D 3433-93 describes a testing procedure to determine the fracture toughness of adhesive bonds between symmetric metallic plates using the double cantilever beam (DCB) and the contoured double cantilever beam (CDCB) test specimens. ASTM standard D 5528-94a extends the DCB method to composite materials. In our work, we have further extended the principles and practices of these two standards to cover the case of an elastic composite layer bonded to a rigid concrete/masonry substrate.

2.5. Modified Beam Theory

The simple beam theory, and the corresponding Equation (8), assumes that the crack front represents a perfect built-in condition. As pointed out in ASTM D 5528-94a, this assumption may not be completely valid in practice, and rotation may occur at the crack front. One way of correcting for this rotation is to apply a modified beam theory (ASTM D 5528-94a) in which the specimen is treated as if it contained a slightly longer debond, a'. The value a' can be determined

experimentally by generating a least square fit of the cube root compliance plot, $C^{1/3}$, as a function of the debond length, a. Hence, the compliance is expressed as

$$C^{1/3} = m \cdot a + n \,. \tag{10.}$$

By setting $a' = a + n/m$, one can use a modification of Equation (9) to write:

$$G = \frac{3m^3(a+n/m)^2 P^2}{2b} \tag{11.}$$

3. TEST SPECIMENS

Test specimens consisted of a concrete substrate and a composite overlay applied on its upper surface. The concrete substrate consisted of a 51-mm × 51-mm × 178-mm (2-in × 2-in × 7-in) concrete brick. The composite overlay was a 3.2-mm (1/8-in) thick and 50-mm (2-in) wide, and consisted of glass fiber reinforced polyester. The concrete brick is manufactured in the USC Civil Engineering and Mechanical Engineering labs using specified equipment and materials. During the brick casting process, two 1/2-in bolts are inserted and set in place (Figure 5b). These bolts attach the specimen to the testing fixture and take up the reaction forces.

During this investigation, 2 sets of specimens were fabricated. The first set consisted of 10 specimens and was fabricated by Dorothy Laub. This first set will be referred to as the D-series of specimens, labeled D1 through D10. The second set consisted of 5 specimens and was fabricated by Shannon Whitley. This second set will be referred to as the "S-series" of specimens, labeled S1 through S5. The second set of specimens was fabricated after the first set was tested and the data was interpreted. Thus, the second set of specimens incorporated the procedural corrections resulting from the fabrication and testing of the first set of specimens.

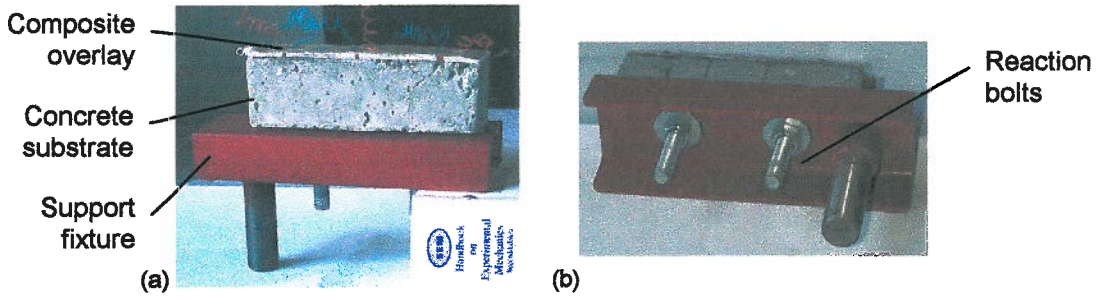

Figure 5 Test specimen developed at USC for testing adhesion strength and fracture toughness between composite overlay and structural substrate: (a) side view showing support fixture, concrete brick and composite overlay; (b) bottom view showing retention bolts (Giurgiutiu, Lyons, and Petrou, 1998).

3.1. Fabrication of Test Specimens

The test specimens were fabricated in stages. First, the concrete bricks were cast and left to cure. After the concrete was cured, the bricks were taken out of the mold and the top surface was prepared for adhesion. Then, surface primer was applied. Finally, the composite overlay was applied through a wet lay-up process. Details follow.

3.1.1. Fabrication of the Concrete Bricks

Six molds were constructed from 12.7-mm (0.5-in.) thick HDPE (Figure 6). The inner dimensions of the molds were 51-mm x 51-mm x 178-mm (2-in. x 2-in. x 7-in.). To one side of the mold was glued an extra piece of HDPE, doubling the thickness of the mold on that side. Through this side of the mold, two ½-in diameter holes were drilled 3-in apart from each other and centered with respect to height and width. Twelve carriage-bolts, ½-in diameter and 3-in long, were placed in the molds so that the head of the bolts were inside the mold and the treaded rods extended through the holes. Nuts were placed on the outside of the mold to maintain the position of the carriage-bolts once the concrete was poured into the molds. Bricks #5 through #10 were fabricate according to the recipe given in Table 2. Bricks #1 through #4 used a similar recipe but with larger-size aggregates.

The solid ingredients were measured out and placed into a large mixing pan: water was measured in a separate container. The water is slowly added to the dry ingredients while ...ring the mixture constantly to achieve even wetting. When the ...ixture attained a dull sheen, it was determined that enough water was added. The concrete was then portioned into the six molds. A vibrator was used to shake the concrete down into the molds and to allow any air bubble to rise to the surface. A straight edge was used to level the concrete and strike it. As the alignment of the bolts is crucial for later insertion in the test fixture, the bolts were checked to verify their straightness. The specimens were covered with moistened burlap and left for 24 hours. After the first day, the bricks are removed from the mold and placed in water where they remain to cure for the remainder of a week.

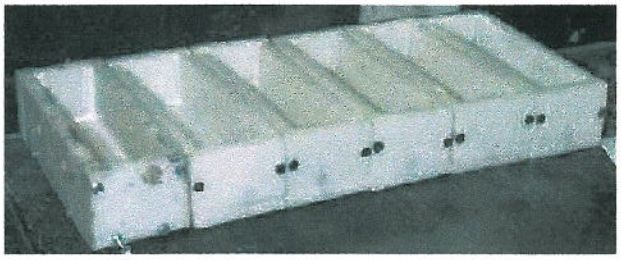

Figure 6 – Molds for the fabrication of concrete bricks.

Table 2 Recipe for the fabrication of concrete bricks #5 through #10

Cement type I	Silica fume	Fly ash	Gravel	Gravel #4	Gravel #8	Sand	Water
1.23 kg (2.72 lbs.)	0.086 kg (0.19 lb.)	0.29 kg (0.65 lb.)	0.95 kg (0.375 in)	1.09 kg (2.4 lbs.)	0.59 kg (1.3 lbs.)	3.23 kg (7.12 lbs.)	1.002 kg (2.21 lbs.)

3.1.2. Surface Preparation

After complete cure of the concrete, the bricks were subjected to surface preparation. The bricks were positioned bolts downward. A steel brush was used to remove the loose dust, particles, and cement paste from the upper portion of the bricks. A vacuum was used to removes loose particles from the surface. The cleaned surface was next primed with Atprime 2A+2B supplied by Reichhold Chemicals, Inc., Durham, NC. Atprime is a reactive polyester polyol that cures in the presence of moisture. To reduce exposure to fumes, primer preparation and application was done under an exhaust hood. The primer was prepared by mixing Atprime 2B with Atprime 2A in the ratio 4:1 w/w. Then, the primer was applied to the cleaned surface of the brick using a hand brush. The primed surfaces were allowed to cure overnight (Figure 7).

Figure 7 - Primed concrete bricks under the exhaust hood.

3.1.3. Fiberglass Preparation

Quad axial glass mat type QM-3408 from BTI Corporation, supplied by Reichhold Chemicals Inc., was used as fiberglass reinforcement. Description of this material is given in Table 3. The material is manufactured from E-glass and stitched together with 135D polyester yarn. Three strips of QM-3408 (cut along the 0^0 direction) were prepared for each brick prior to mixing the resin with the initiator. The dimension of these strips matched the dimensions of the brick top surface (51-mm x 178-mm; 2-in x 7-in). The outline of the strips was drawn onto the fiberglass cloth prior to being cut. The cut strips were divided into stacks of three and set aside.

Table 3 Description of the Quad axial glass mat type QM-3408 from BTI Corporation (oz/sq. ft.)

Specific weight	0^0 direction	90^0 direction	$+45^0$ direction	-45^0 direction	Random 2-in chopped mat
g/m^2	3.93	2.75	1.98	1.98	2.06
oz/ft^2	13	9	6.5	6.5	6.75

3.1.4. Priming of the Piano Hinges

In order to introduce the load at the tip of the composite layer, piano hinges were used. One hinge was needed for each specimen. The hinge was 51-mm (2-in) long and had two 6.3-mm (0.25-in) holes one each side. When purchased, the hinge came in plastic wrappers. Upon the wrapping being opened, the hinge was found slightly greasy. We used sandpaper

to roughen up the metal surface of the hinges and to remove any protective coating. Then, the hinges were degreased with ethyl alcohol and subjected to surface conditioning using Micro Measurements, Inc. (Rayleigh, NC) products. M-prep Conditioner A was applied repeatedly using a fine-grit wet-and-dry abrasive paper. During this process, the hinge was cleaned with paper towels until no discoloration was observed on the paper towel. This step was followed by rinsing the hinge with distilled water. Then, the clean surface was dried by a single slow stroke with the paper towel. M-prep Neutralizer 5A was applied to the clean surface. This way, the bonding surfaces of the hinge were prepared for good adhesion with the resin. In order to prevent lockup of the hinge due to the resin absorption, the pin of the hinge was locally greased. In this process, care was taken not to contaminate the rest of the conditioned hinge.

3.1.5. Application of the Composite Overlay

The composite overlay was applied using a wet lay-up process. Atlac 580-10 polyester resin and 46747 peroxide initiator (MEKP type) were used to create the composite matrix material. This resin also served as the adhesive between the composite overlay and the concrete substrate. Both ingredients used in the resin preparation were supplied by Reichhold Chemicals, Inc. The peroxide initiator was thoroughly mixed with the resin (1:80 w/w ratio) in a hand-mixing vessel. Because the gel time of the resin is 25 minutes, it was found that the best to mix enough resin for no more than 6 specimens at a time. The initiated resin was painted onto the brick surface using a disposable paint roller. The first fiber glass section was placed over the surface and a metal roller was used to impregnate the fibers with the resin. Then, a second layer was applied through the same process. After the second layer was applied, the primed metal hinge was placed at the end of the specimen with the rounded pin-side facing downwards. The third and final layer was positioned on top of the specimen, the impregnation process was repeated. This way, the metal hinge was incorporated between the second and the third composite layers. A final coating of resin was rolled onto the surface using the disposable paint roller. This procedure was repeated for all of the specimens. The composite was allowed to cure under normal room temperature and humidity conditions (Figure 8). The composite seemed fully cured and cool to the touch within 2-3 hours after completion. To ensure complete cure, at least 24 hours were left to pass before the specimen was taken to the next stage.

Figure 8 - Apply Composite Overlay

3.1.6. Specimen Pretest Preparation

The pretest preparation of the specimen consisted of removing the fiber/resin spill-out, dressing the side surfaces, initiating the crack, and applying the crack read-out ruler. The fiber/resin spill-out was removed from the sides of the specimen using a hand held hacksaw. During this process, the brick was held in a bench vice. After any overhanging composite was completely removed, a metal file was used to smooth down the sides, increasing the visibility of the bond region. Both the hacksaw and file operations were done in such a way as not to induce unwanted cracks in the specimen at the overlay/substrate interface. Next, a razorblade was used to initiate the crack at the hinge end of the specimen. The razorblade was prepared for this operation by removing the backside attachment of the blade such that only the flat side with a sharp edge remained. The brick was placed in a vice to arrest the crack growth beyond the under-the-hinge perimeter. Then, the razor blade was tapped into the specimen, between the composite and the brick, to induce a pre-crack the interface. (For the fist two specimens, we used Teflon strips placed in the overlay/substrate interface, just under the hinge. In the remaining 8 specimens, we used the razorblade method which, we believed, resulted in a sharper pre-crack than with Teflon strips.) To facilitate observation of crack propagation during testing, the interface between the composite overlay and the concrete brick substrate was painted with white water-based typewriter correction fluid. A paper ruler was glued to both sides of the brick just below the paint line. The specimen number and date were written on the specimen with a permanent marker and photographs were taken with a digital camera.

3.2. Tests

3.2.1. Experimental Setup

The experimental setup consisted of an MTS 810 Test System fitted with an 890-N (200-lb) load cell and loading fixture (Figure 8). The MTS 810 Test System is controlled through a National Instruments Labview interface card and programming language installed on a Gateway 2000 lab PC. Labview was used to run the test and gather data. Data was collected through the Labview interface and brought into the PC for processing. The loading fixture was first mounted on the ram head of the MTS 810 Test System. The specimen was mounted onto the loading fixture with the bolts protruding downward through the holes. A rubber pad was positioned between the brick and the fixture to prevent damaging the specimen while being tightened to the fixture. A tongue and clevis joint fixture was used to connect the load cell to the specimen. The tongue was bolted to the piano hinge attached at the end of the specimen. The clevis was fixed into the load cell end. Good alignment of the two pieces was verified, and fine adjustments were applied, as necessary.

3.2.2. Test Procedures

The test procedure followed the general rules laid out in the ASTM standards for DCB testing (ASTM D 3433-93 and 5528-94a). The specimen was loaded monotonically under displacement control at a ram rate of 0.13-mm/sec (0.005-in/sec). During loading, the load and displacement values, and the load-displacement curve were displayed in real time. When the load value was observed to drop, or when the crack was observed to grow, the loading was paused, and the crack was allowed to propagate under constant displacement. When the crack propagation was completed and the crack was arrested, the crack length was measured, and the current values of crack length, load, displacement, and time were recorded to the data file. Then, the loading restarted, and the process was repeated until complete delamination was achieved. Complete delamination was assessed by load dropping to zero and crack extending along the entire length of the specimen. Photographic documentation was performed during and after the test. Post test photos of the fracture surfaces were carefully taken in order to assess the nature of the disbond.

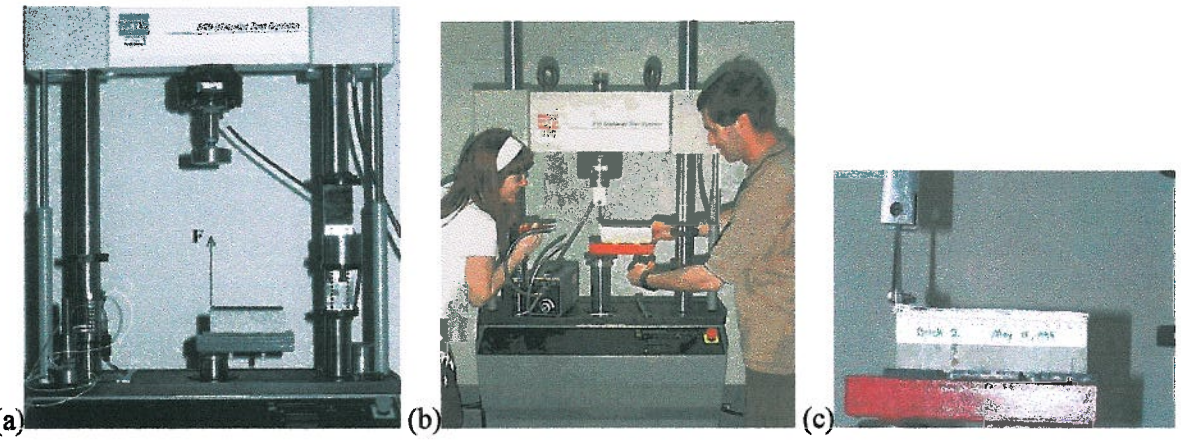

Figure 9 Experimental setup for determining the fracture toughness of the bond between the composite overlay and the concrete substrate: (a) test machine and specimen indicating the loading direction; (b) mounting of specimen #1; (c) close up view of the specimen #2 showing the eye and clevis joint fixture.

4. POST TEST PROCESSING

4.1. Evaluation of the Specimens

The specimens were evaluated visually in terms of (a) appearance of the composite; (b) appearance of the fracture surface; and (c) type of crack propagation, i.e., in the interface or in one of the constituents. In general, it was observed that crack propagated in a mixed fashion, partially through the upper layer of the concrete substrate, and partially in the interface between the concrete and the composite. When the crack propagated through the upper layer of the concrete substrate, cement paste residue was observed on the matching surface of the composite overlay. When the crack propagated through the interface, the two crack surfaces had no cement-paste residue and had a glossy appearance. The

percentage of the fracture surface that was covered with cement paste residue was measured and recorded (Table 4). Details follow.

4.1.1. Evaluation of the D-Series Specimens

Specimen D1: The crack first began to grow at the hinge within the composite. As the crack continued, it quickly switched to the bonded region between the composite and the concrete. Failure occurred at the concrete/composite interface. Approximately 80% of the fiberglass composite overlay portion was covered by a very thin layer of cement paste. The bolts were tightened to the fixture in excess to the limit and the brick cracked at the bolt. For this reason, measurements beyond 100-mm were not used in the data processing.

Specimen D2: No cement paste was observed on the first 30-mm from the pre-crack. The following 50-mm of the fiberglass composite did exhibit good bonding between the composite and the cement paste. Approximately 26% of the total surface was covered with the cement paste. The white out that had been painted onto the specimen prior to testing was observed to have penetrated deeply into the specimen (2-mm) suggesting that there might have been voids along the edge.

Specimen D3: The hinge in the composite of this specimen was not positioned properly as a result of slipping while the resin was still gelling. In addition, some caulk remained on the specimen from the molds. The crack was observed to initiate from the razor blade that was used to pre-crack the specimen. As the crack began to grow, the composite was observed to bend, but this was an elastic deformation. The white out did not penetrate deeply into the sides as it did on the second specimen, possibly indicating that there were fewer voids. However, the cement paste did not bond to the composite portion of the specimen. The fracture surface on both sides was predominantly glossy with only 17% of the total surface covered with cement paste.

Specimen D4: The crack initiated at the razor's edge. During the test, the crack was observed to propagate with no decrease in the load. The crack continued to propagate through the materials while the RAM position was held constant. The load dropped accordingly. The composite was observed to bend during the test. Again, this was elastic deformation. The surface of the composite was very glossy with only 7% of the total surface area covered with cement paste, and there re fibers in the composite that did not appear to be fully wetted by the resin.

Specimen D5: There appeared to be better adhesion along one side of the specimen. This side was covered with a thin layer of concrete paste. There were many resin bubbles protruding from the surface on the side of the composite overlay that had more cement paste adhered to it, accounting for 41% of the total surface area.

Specimen D6: The third of composite overlay nearest the hinge was fibrous, as if the glass fibers had not been fully wetted. Cement paste was observed on approximately 17% of the surface area along one edge of the overlay. The rest of the overlay was glossy.

Specimen D7: A fibrous region extending from the hinge to approximately a quarter of the length of the composite overlay was observed. A narrow glossy region was observed along the center of the overlay, and cement paste was observed all along the sides of the brick. In the regions where cement past was observed, there were resin bubbles protruding out of the overlay into the brick where the resin had filled some voids on the surface of the brick. These regions accounted for 53% of the surface area.

Specimen D8: Much of the surface of the overlay was fibrous. The fibrous regions were along the center of the brick whereas the outer edges of the overlay were covered with a thin layer of cement paste. The portion of the overlay that was covered in the cement paste was approximately 57%.

Specimen D9: Closest to the hinge, the composite overlay is fibrous. The edges had a layer of cement paste and the center was glossy. White out penetrated into the specimen as much as 8-mm (0.31-in). Only 34% of the surface area was covered with the cement paste.

Specimen D10: This composite overlay appeared to be fully wetted, though lighter in color near the hinge. The overlay was observed to be divided along the center through the length of the specimen. One side was covered with concrete paste and the other appeared to be glossy. The paste region accounted for 38% of the total surface area.

Table 4a Percentage of fracture surfaces retaining cement paste in the first set of specimens

Specimen #	D1	D2	D3	D4	D5	D6	D7	D8	D9	D10
Percentage of fracture surface retaining cement paste	80%	26%	17%	7%	41%	17%	53%	57%	34%	38%

4.1.2. Evaluation of the S-Series Specimens

Specimen 1: From the hinge, the crack grew in the concrete/composite interface along the edges of the specimen. Concrete paste along the outer edges protruded 20 to 23-mm toward the center of the specimen (Figure 10). The mid-region of the specimen retained the primer resin; thus, the crack did not propagate along the concrete/composite interface. In areas where the concrete surface seems to have crevices where resin settled in larger amounts, larger portions of cement paste were retained on the removed composite layer. At a crack length of 55-mm, cement paste is present along the mid-section of the specimen, generally where the concrete surface had more voids or crevices. The hinge was not straight, due to slipping before the resign cured; this is a possible reason for the larger amount of concrete paste on the left side of the composite (see picture to the right). 45% of the composite surface held concrete paste.

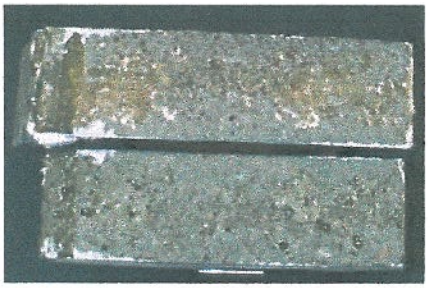

Figure 10 Specimen 1 interface

Specimen 2: Crack propagation occurred as it did in the Specimen 1. The crack grew in the concrete/composite interface along the edges of the specimen (Figure 11). The hinge was slightly off center, due to slipping during lay-up. The top edge retained more concrete, protruding 28-mm toward the center of the specimen, initially. In this region, aggregate was also removed from the top surface of the concrete. When the crack propagated to 60-mm from the hinged edge, concrete paste can be observed as occupying the entire cross section of the composite surface for 40-mm. After this region, the concrete paste resides along the edges of the composite, where more aggregate was removed. 60% of the composite surface contained concrete paste.

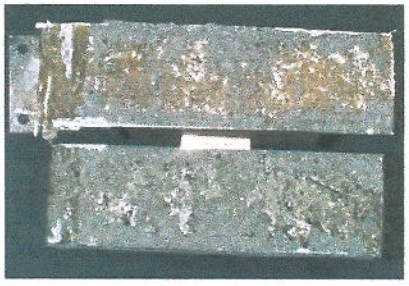

Figure 11 Specimen 2 interface

Specimen 3: Concrete paste is present over the entire cross-sectional area of the initiated crack (Figure 12). The concrete paste is not present on the composite surface where large crevices are present in the concrete specimen. In these areas, large pools of composite primer were allowed to accumulate. These locations are distinguishable in the photograph to the right. In the areas to the far right of the specimen, these large resin pools are adjacent to large amounts of removed aggregate. Like the other specimens, this specimen shows that larger amounts of concrete paste were removed along the edges of the specimen. 93% of the composite surface retained concrete paste.

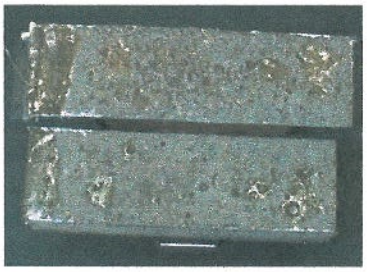

Figure 12 Specimen 3 Interface

Specimen 4: Concrete paste was removed uniformly in the initial crack propagation. When the crack grew to 30-mm from the hinged edge, less concrete paste was detached due to resin pools in the concrete surface (Figure 14). In these areas, the strength of the resin was tested instead of the bond strength. Following these regions, the concrete paste returned to its uniform distribution across the composite surface. When the crack reached 85-mm from the hinged edge, another resin pool was contacted. This particular resin pool contained air pockets that helped enable the removal of concrete from this particular area. Other locations that behaved similarly are located at 122-mm from the hinged edge and at 172-mm. 95% of the composite surface was covered with cement paste.

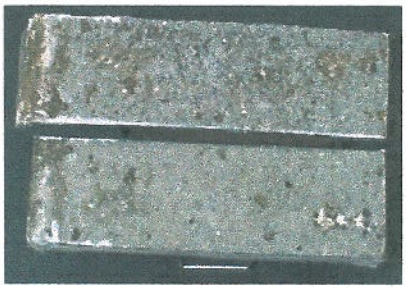

Figure 13 Specimen 4 Interface

Specimen 5: Crack propagation was uniform throughout the concrete/composite interface, accounting for 98% of the composite surface being covered with cement paste (Figure 14). Areas that did not retain paste were located over large crevices in the concrete surface where large amounts of resin had settled. Also areas that did not retain concrete were located immediately after a large portion of concrete paste had been removed from the concrete surface.

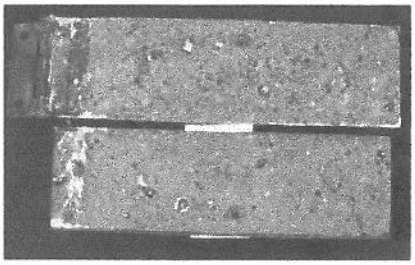

Figure 14 Specimen 5 Interface

Table 4b Percentage of fracture surfaces retaining cement paste in the second set of specimens

Specimen #	S1	S2	S3	S4	S5
Percentage of fracture surface retaining cement paste	45%	60%	93%	95%	98%

4.2. Data processing

The data files collected during the tests were processed using MS Excel software. First, load-displacement graphs were produced. These graphs clearly indicated the loading cycles and the crack propagation regions. Next, plots of the cubic root of compliance *vs.* crack length were generated and a least-squares straight line fit was applied. These graphs correspond to equation (10) and generate the m and n values necessary for the calculation of SERR, G, with Equation (11). In producing these fits, attention was paid to the elimination of outliers that would distort the results. Finally, the fitted m and n values were used in Equation (11) to generate graphs of SERR, G, *vs.* crack length, a. The results of data processing are presented in Figure 10. Three graphs are presented for each specimen: (a) the as-recorded load-displacement plot; (b) linear fit between the cubic root of compliance, $C^{1/3}$, and the crack length, a; and (c) the plot of strain energy release rate, G, as function of crack length, a. The $C^{1/3}$–a plots show very little scatter and indicate a good linear fit of the data and confirm the soundness of the experimental method. The G–a plots show some data scatter. The arithmetic mean value of G for each specimen was superpose on the G–a plots.

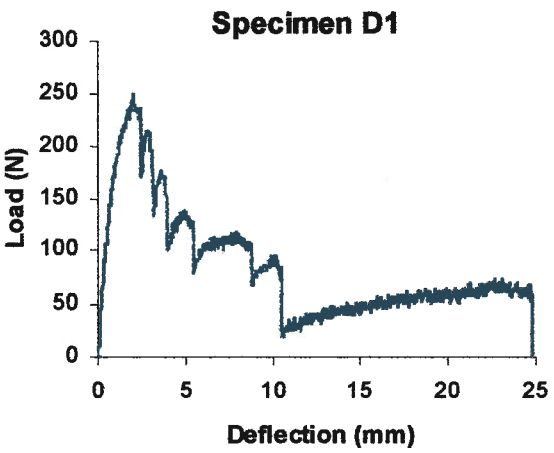

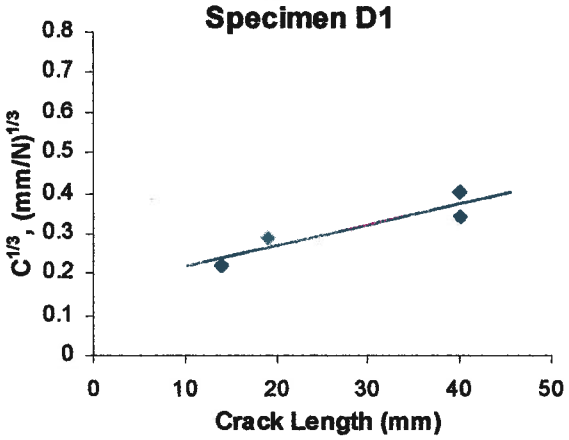

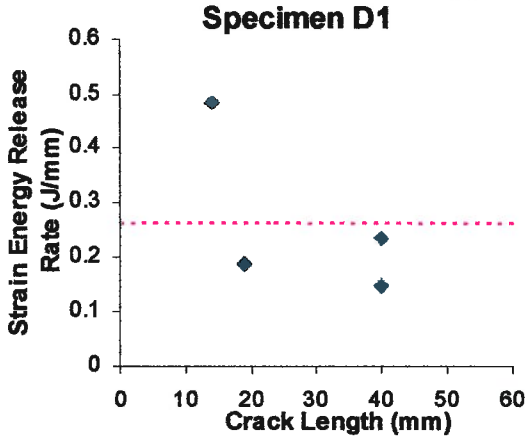

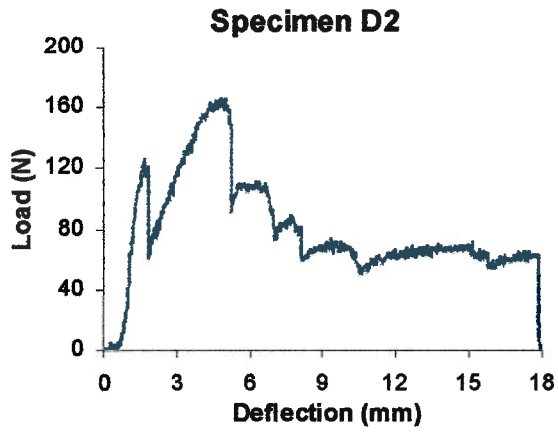

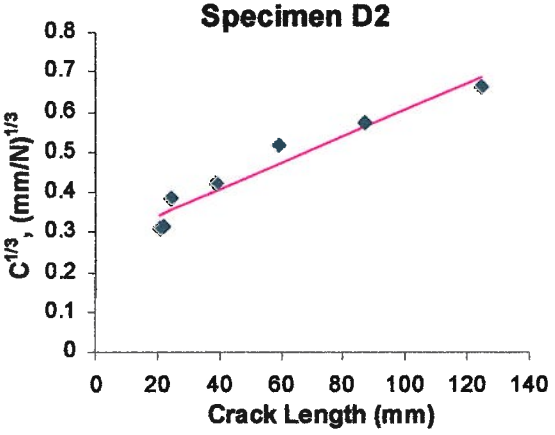

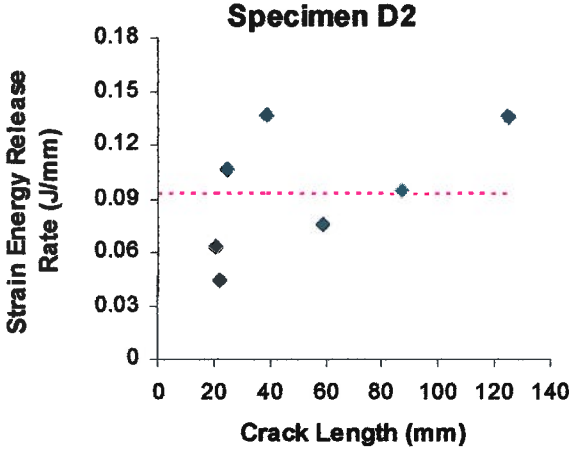

Figure 15 Results of data processing, grouped by specimen numbers

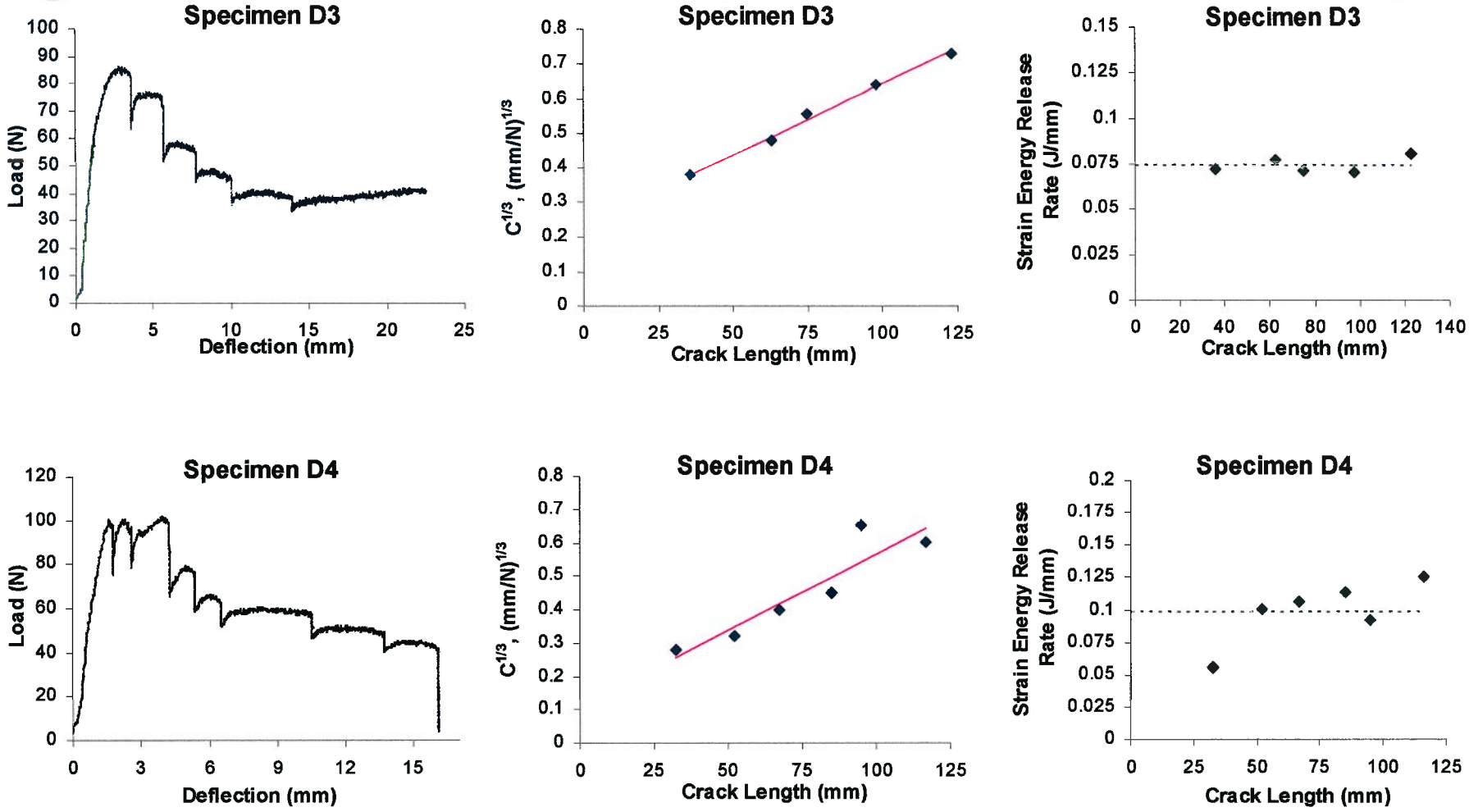

Figure 15 Results of data processing, grouped by specimen numbers (cont.)

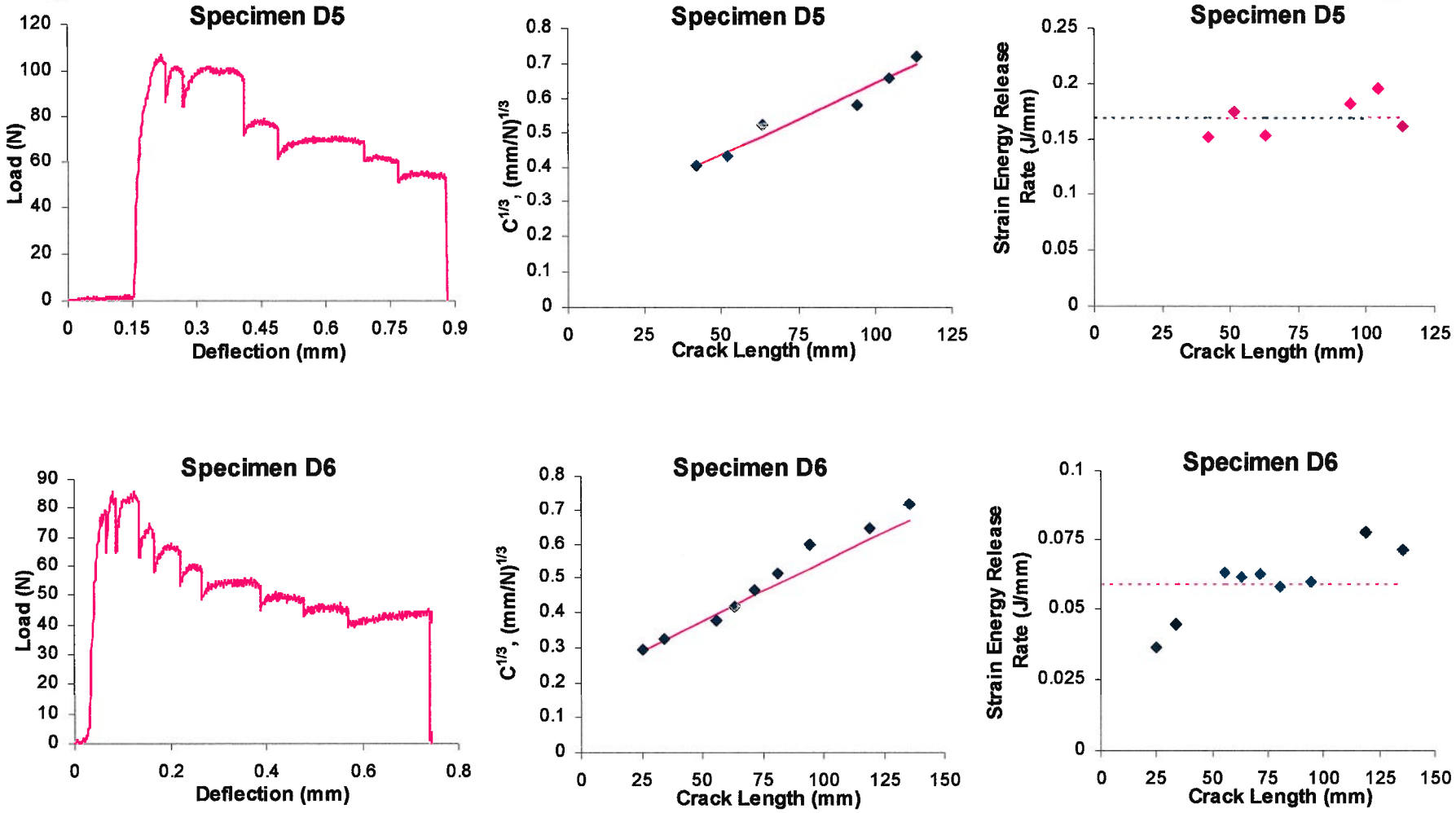

Figure 15 Results of data processing, grouped by specimen numbers (cont.)

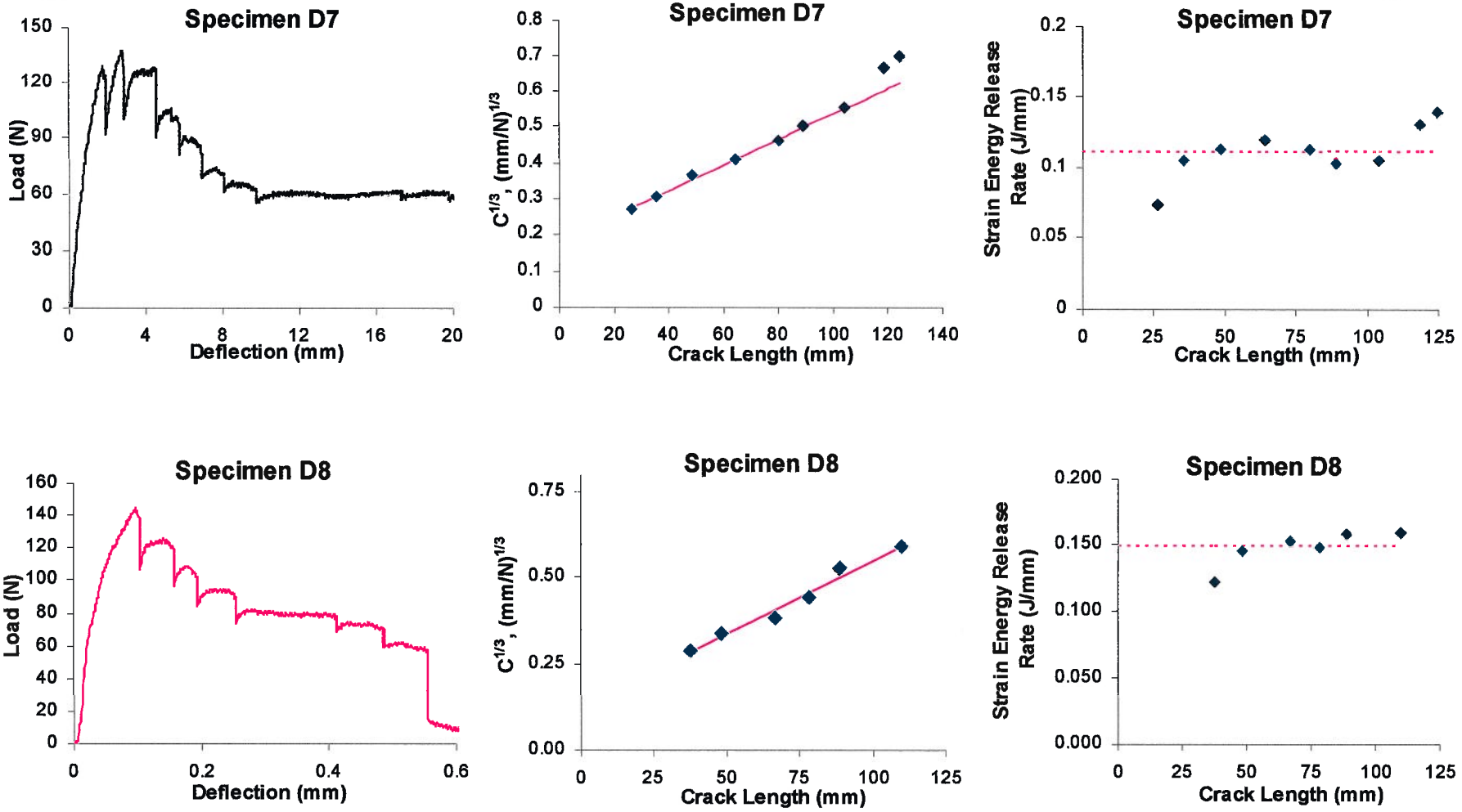

Figure 15 Results of data processing, grouped by specimen numbers (cont.)

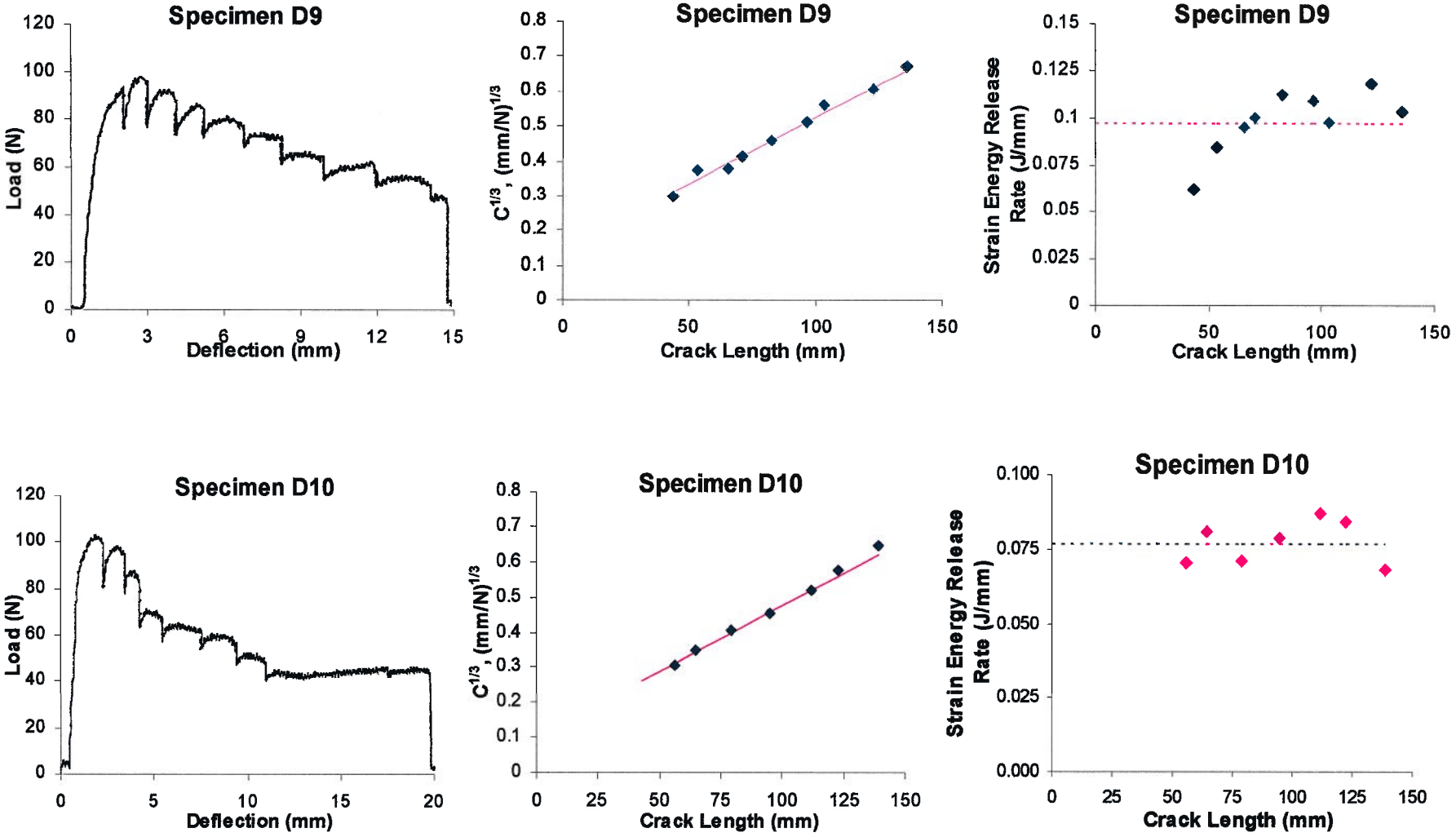

Figure 15 Results of data processing, grouped by specimen numbers (cont.)

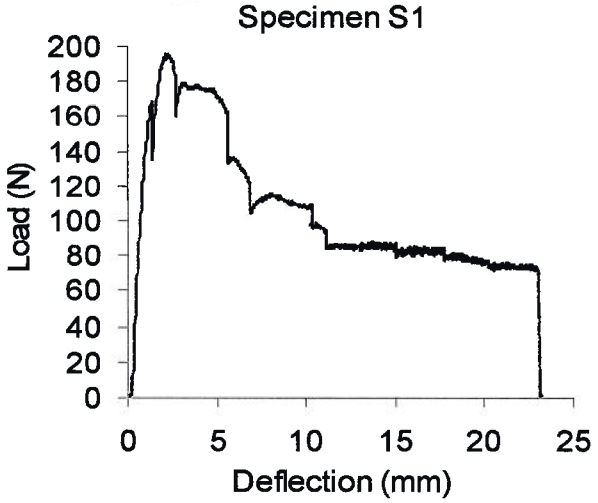

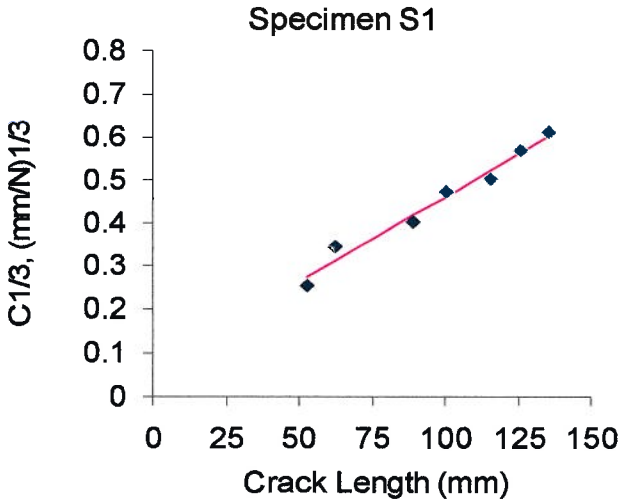

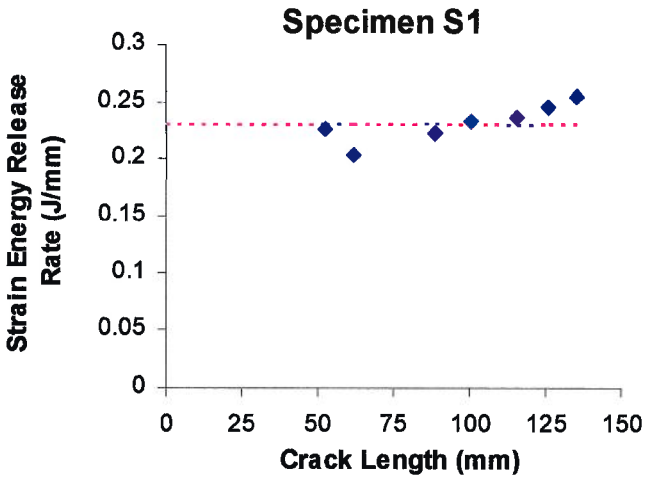

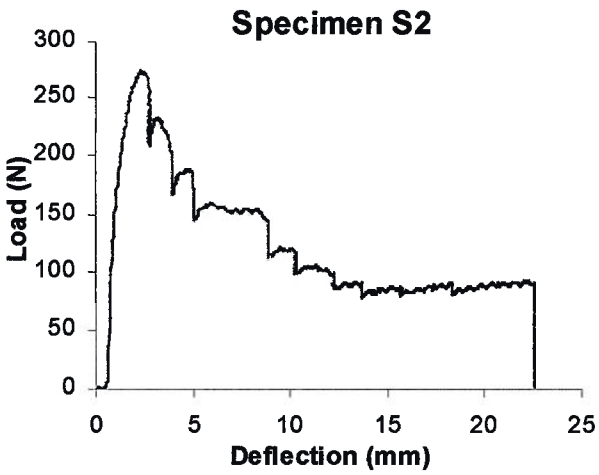

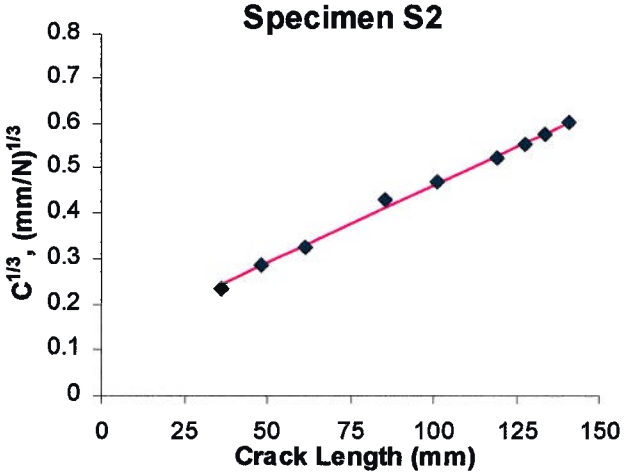

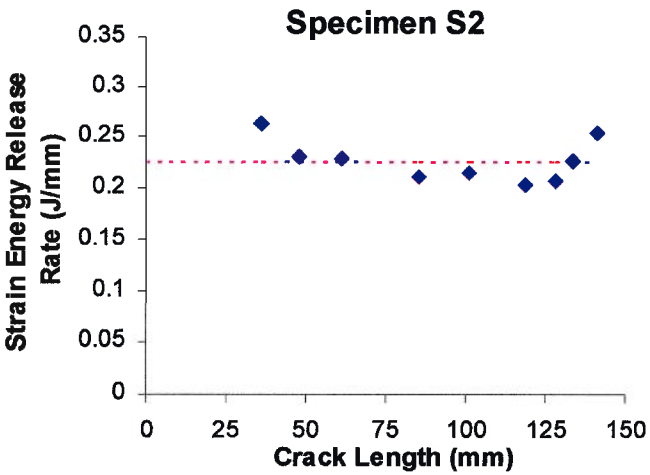

Figure 15 Results of data processing, grouped by specimen numbers (cont.)

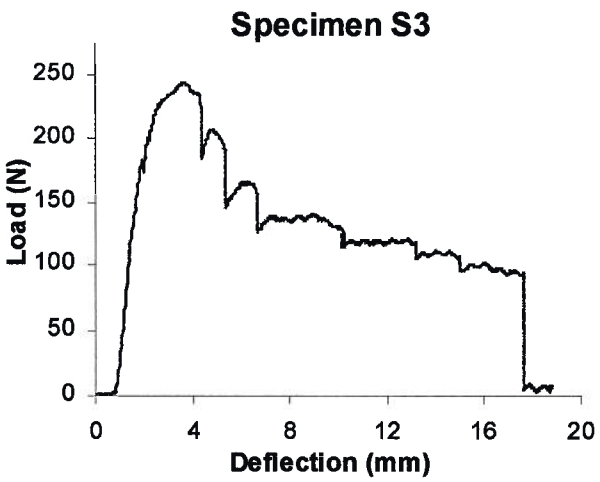

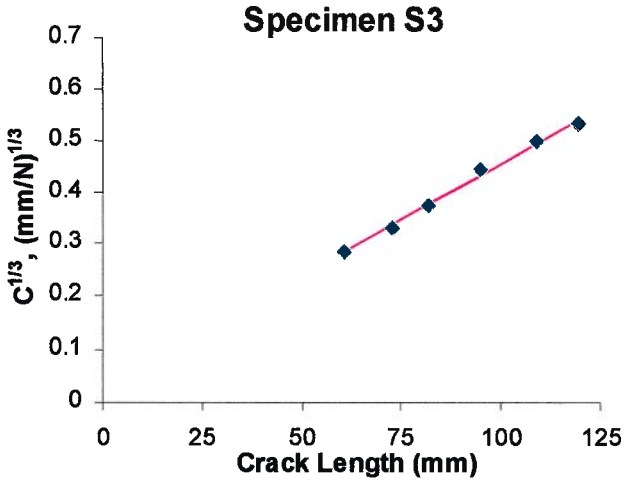

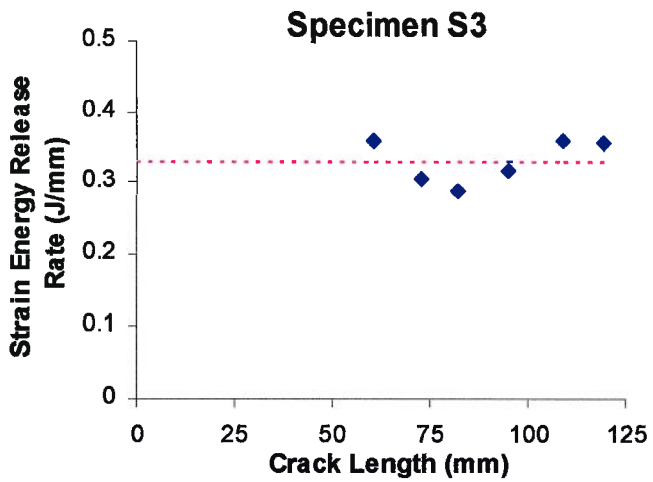

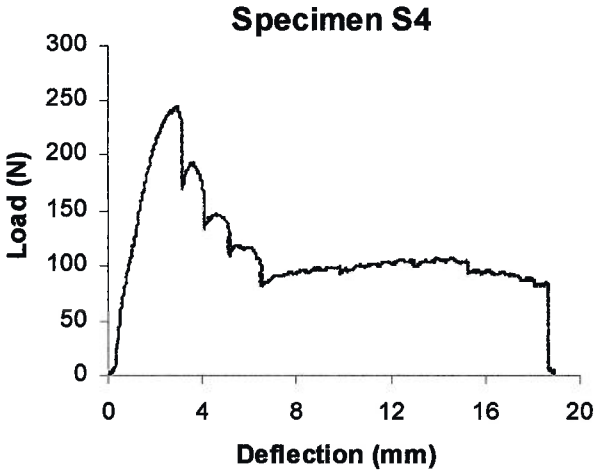

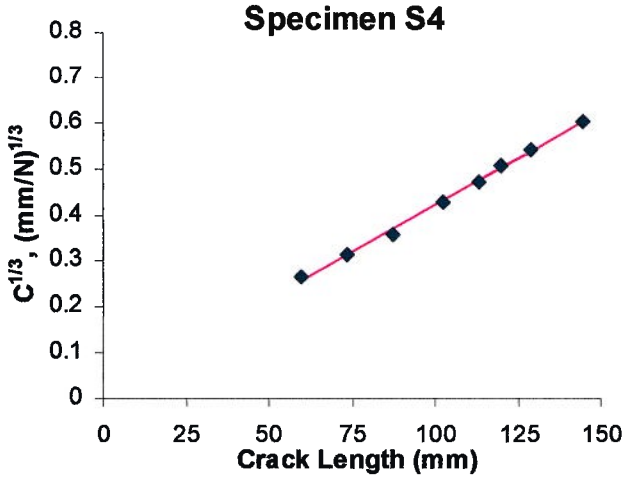

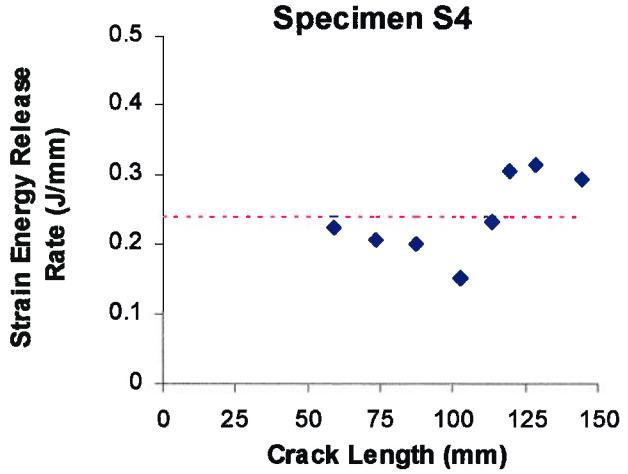

Figure 15 Results of data processing, grouped by specimen numbers (cont.)

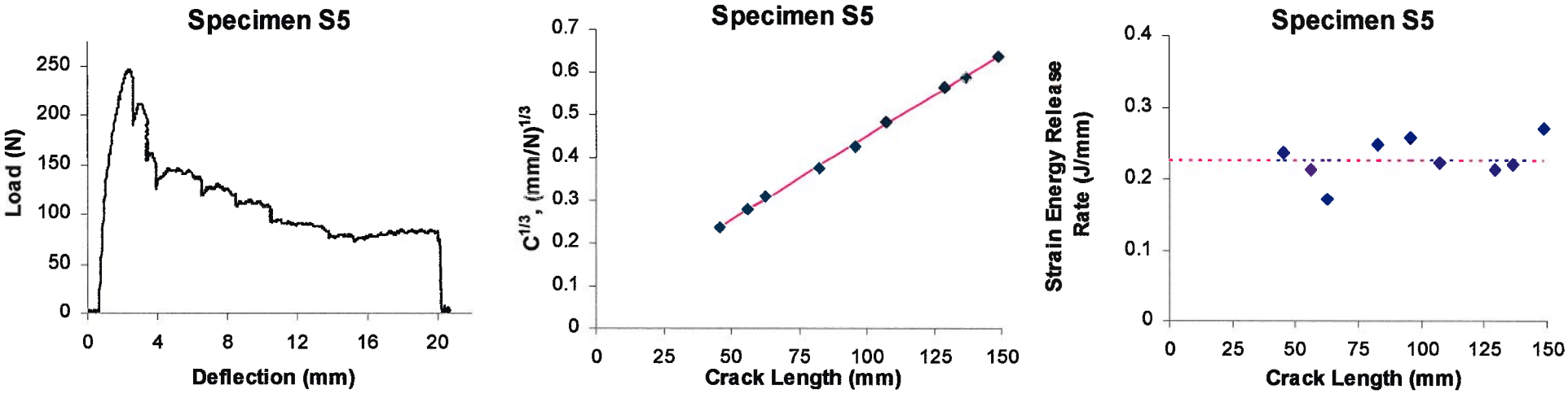

Figure 15 Results of data processing, grouped by specimen numbers (cont.)

5. DISCUSSION OF TEST RESULTS

5.1. Discussion of the Test Results for the D-series Specimens

Table 5 gives the mean values of strain energy release rate (SERR) resulting for the testing of the ten D-series specimens. A plot of these results, ordered by increasing SERR values is given in Figure 11a. Examination of Figure 11a reveals that most of the specimens displayed a mean SERR value around $G_{average}$ = 0.1 J/mm. Some specimens (e.g., #3 and #6) displayed a value less than 0.1 J/mm. Other specimens (e.g., # 5 and #1) displayed a value well above 0.1 J/mm. Our contention is that the value $G_{average}$ = 0.1 J/mm could be considered as an average value for the first set of specimens. However, some discussion of the outliers is useful to understand (a) the causes of reduced toughness of the bond between composite and concrete; and (b) ways to improve the fracture toughness and strengthen the composite/concrete bond.

Table 5 Strain energy release rate values

Specimen #	1	2	3	4	5	6	7	8	9	10
Average Value of Strain Energy Release Rate (J/mm)	0.265	0.094	0.075	0.099	0.171	0.059	0.111	0.115	0.098	0.077

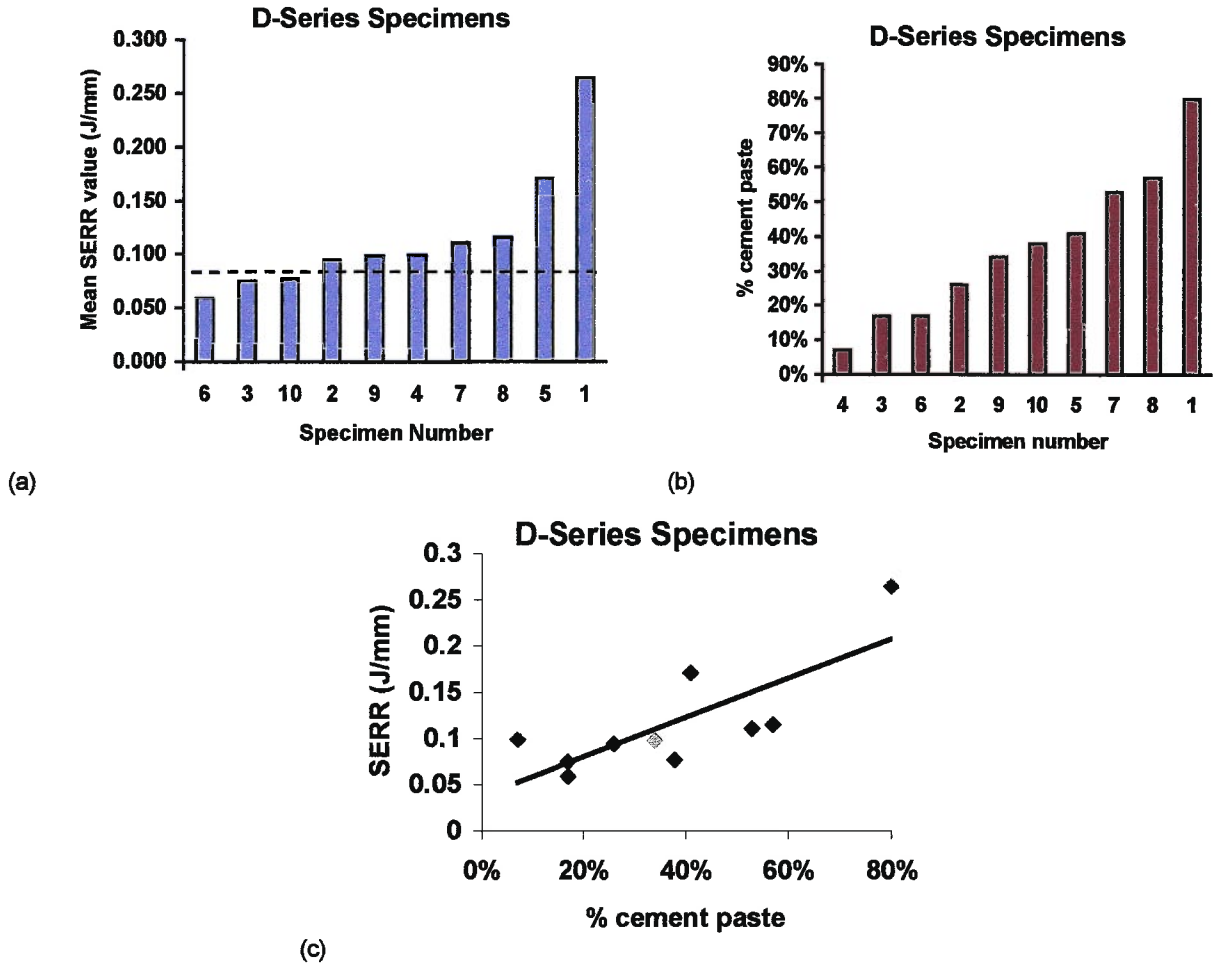

Figure 16 Synoptic representation of the test results sorted out in ascending order: (a) mean strain energy release rate (SERR) values; (b) percentage of fracture surface presenting cement paste retention (c) correlation between mean SERR and % cement paste.

D-Series Specimens with Higher-than-average SERR: Specimens #1 and #5 showed a higher-than-average SERR. This means that the adhesion fracture toughness of these specimens was better than of the rest. Why would this happen?

Examination of data for specimen #1 indicates that this specimen also had much larger levels of load during the test. This indicates an overall stronger adhesion. The percentage of fracture surface retaining cement paste after fracture is also highest in this specimen (Figure 11b). This indicates that a good bond was created between the composite and the substrate during the wet lay-up process. Thus, when cracking took place during the test, the crack was forced to propagate in the concrete substrate. Since the cement paste present in the upper layer of the concrete substrate is weaker than the rest of the concrete, the crack propagation was took place in the cement paste layer. As shown in Figure 11a, this type of crack propagation yields the highest fracture toughness. Examination of specimen #5 also shows a significant percentage of the fracture surface being covered with concrete paste (Figure 11b). However, the ranking of specimen #5 in terms of the percentage of concrete paste coverage on the fracture surface is lower than its ranking in terms of fracture toughness. This indicates that the percentage of concrete paste coverage on the fracture surface is not the only indicator of a strong bond, and that other factors (confounders effect and/or modifiers) are involved.

D-Series Specimens with Lower-than-average SERR: Specimens #3, #6, and #10 had lower-than-average strain energy release rate values (Figure 11a). Of these, specimens #3 and #6 are also the specimens with the lowest percentage of concrete paste coverage of the fracture surface. From this point of view, these specimens confirm that a significant correlation exists between the fracture toughness and the percentage of cement paste coverage of the fracture surface. On the other hand, specimen #10 has a different behavior. Its ranking in terms of the percentage of cement paste coverage of the fracture surface is higher than its ranking in terms of fracture toughness. This observation proves again that, though a significant correlation exists between bond fracture toughness and percentage of cement paste coverage left on of the fracture surface, other factors, confounders effect and/or modifiers, are also involved.

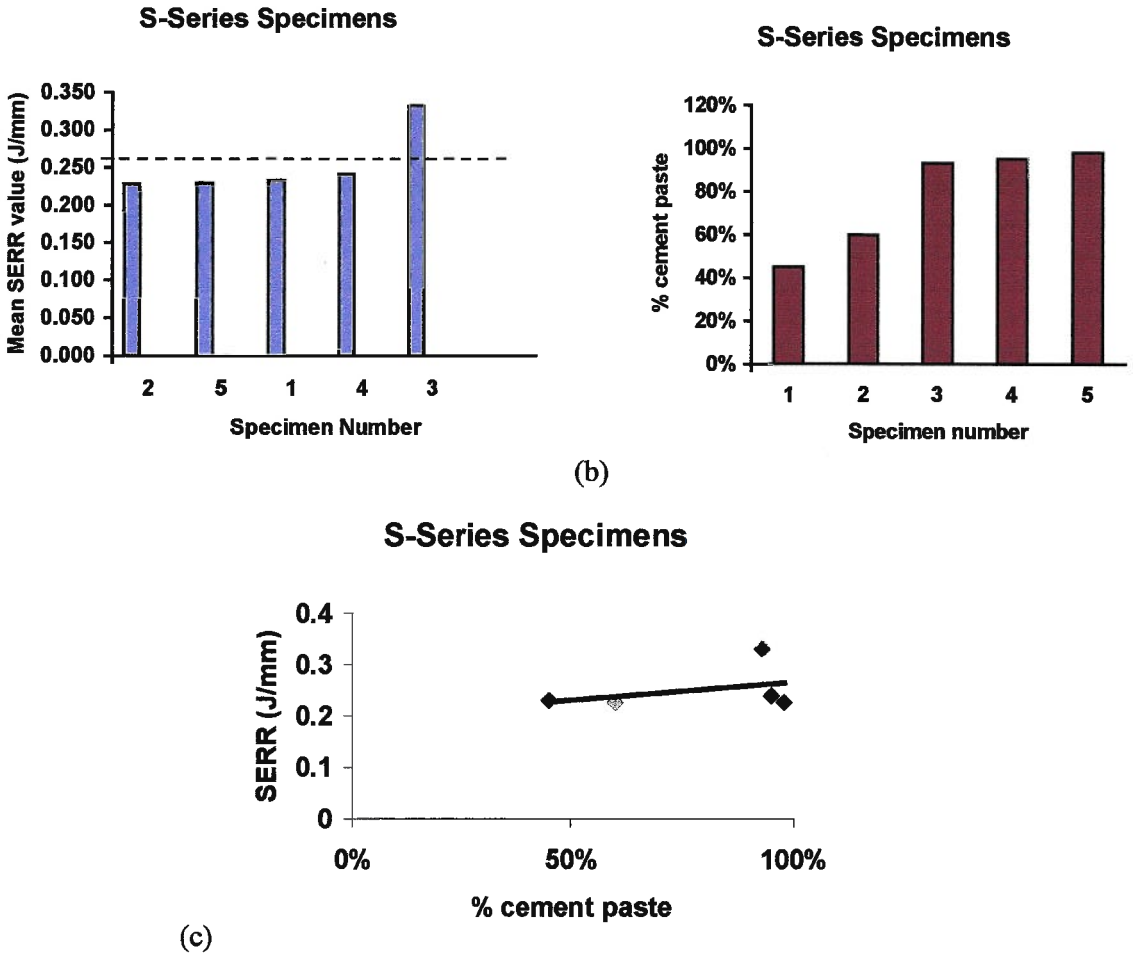

Figure 17 Synoptic representation of the test results sorted out in ascending order: (a) mean strain energy release rate (SERR) values; (b) percentage of fracture surface presenting cement paste retention; (c) SERR vs. percentage cement paste.

5.2. Discussion of the Test Results for the S-Series Specimens

Table 6 gives the mean values of strain energy release rate (SERR) resulting for the testing of the five S-series specimens. A plot of these results, ordered by increasing SERR values is given in Figure 11a. Examination of Figure 11a reveals that most of the specimens displayed a mean SERR value around $G_{average}$ = 0.252 J/mm. Some specimens (e.g., #3 and #6) displayed a value less than 0.1 J/mm. Other specimens (e.g., # 5 and #1) displayed a value well above 0.1 J/mm. Our contention is that the value $G_{average}$ = 0.252 J/mm could be considered as an average value for the second set of specimens. However, some discussion of the outliers is needed to understand (a) the causes of reduced toughness of the bond between composite and concrete; and (b) ways to improve the fracture toughness and strengthen the composite/concrete bond.

Table 6 Strain energy release rate values

Specimen #	S1	S2	S3	S4	S5
Average Value of Strain Energy Release Rate (J/mm)	0.232	0.228	0.332	0.241	0.229

5.3. Correlation of Strain Energy Release Rate with Percentage Cement Paste Retention on the Faying Surfaces

A sample-to-sample variation in SERR values of approximately one order of magnitude was observed. This variation is related to differences in the fracture paths in the samples. The fracture surfaces of all samples had areas where cement paste adhered to the composite overlay after it was peeled off, indicative of good adhesion between the composite and the substrate in these areas. However, there were also regions where the cement was not adhered to the overlay, indicating poor adhesion and/or pre-existing voids at the composite-to-concrete interface. The relative amount of cement paste adhered to the overlays varied significantly among the samples.

The amount of cement paste adhered to the overlay was quantified by measuring its area percentage using a statistical point counting method. When SERR is plotted against the percentage of cement paste adhered to the overlay, as in Figure 18, it is clear that a correlation exists. In this figure, the data and the regression line show that SERR increased with an increased amount of cement paste adhered. The r^2 statistic of the regression line was low, however (r^2 = 0.65), due to several outliers. For example, three samples with % cement paste values between 40 and 60% fell below 1 standard deviation of the regression line. Closer examination of the fracture surfaces of these samples indicates that they had large debond areas, whereas the debond areas on the other samples tended to be smaller and more equally distributed on the surface. On one of these samples, one side of the overlay was almost bare of cement paste but the other side was almost completely covered with it. While the trend of increasing SERR with increased percentage of cement paste adhered exists, these observations indicate that the distribution of the debonds also plays an important roll in determining the effective toughness of the composite-to-concrete bond.

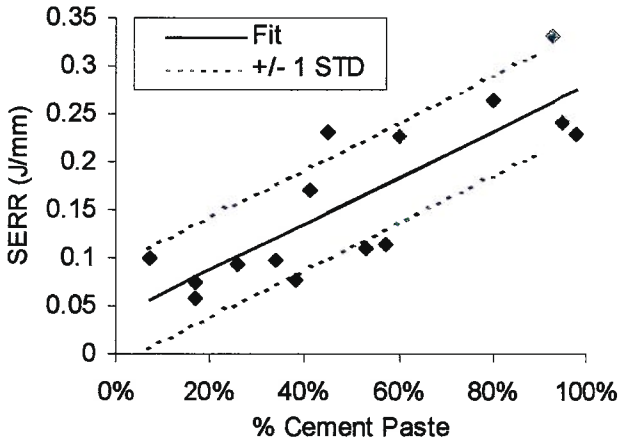

Figure 18 Correlation of strain energy release rate (SERR) with percentage cement paste retained on the faying surfaces after debonding

Variation in the results is likely associated with the hand lay-up procedures used to fabricate the specimen. Poor adhesion could be related to the time elapsed between applying the primer and the composite, or to the resin being applied late after mixing, while it started to gel. Differences in the distribution of the poorly adhered areas could be attributed the inexperience of the personnel (student assistants) who fabricated the test specimens. This underscores the importance that training, experience and quality control will have when composite materials are applied to civil engineering structures in the field.

5.4. Sources of Error and Variability

The sources of error and variability involved in this experiment fall mainly into two categories: (a) variability connected with specimen fabrication; and (b) errors connected to the test procedure and data processing. It is the authors' opinion that the variability connected with specimen fabrication greatly exceeds the errors that might have been introduced *via* test procedure and data reduction. Variability in specimen fabrication is reflected in the fracture surface differences observed during the post-test examination of the specimens. Thus, some specimens retain a large proportion of concrete paste on the composite side of the test specimen, while others presented a fracture surface with a glossy aspect. The glossy surface aspect indicates poor adhesion between the basic ingredients – resin, primer, and concrete. This situation could be due to the resin being applied too late after mixing, while it started to gel. It can also be due to too much time being allowed to elapse between the application of the primer on the concrete substrate and the application of resin on the primed surface. (Reichhold Chemicals Corporation specifications indicated that the Atprime should be allowed to moisture cure for approximate 1.5 hours before the polyester resin is applied, while in our work this period was 24 hours.) This variability in specimen fabrication is explainable and attributable to the lack of specific training experience of the personnel involved in the manufacturing of the specimens. In our case, undergraduate students with practically no experience in handling composite materials were used. Only specimen #1 was manufactured and tested under the direct supervision of a faculty member (the first author). The fact that its fracture toughness is more than twice larger than the average value for the complete set indicates the importance of quality control during the fabrication of composite specimens.

Other sources of error, that might have affected the results, could be connected with the irregular placement of hinges and with the different volume fraction of resin in the composite overlay. The hinges may not have been placed exactly in the same manner, thus allowing the crack to propagate in a different direction for each of the specimens. However, a gross difference in crack propagation was not observed during the tests. Different amounts of resin in the composite from sample to sample may have caused some discrepancy in the overlay stiffness. But the composite stiffness did not enter the calculations that were based on the compliance method alone.

6. CONCLUSIONS

The aging of US infrastructure is posing serious problems to the engineering community. To offset the high cost of direct replacement, repairs, upgrade, retrofit, and rehabilitation schemes are currently being considered. Composite overlays are attractive materials for such applications, but their in-service behavior is insufficiently known. To address these issues, the College of Engineering of the University of South Carolina has formed an interdisciplinary team for experimental and theoretical research. Studies are planned at coupon, scaled components and full-scale levels. Bond strength, fracture toughness, crack propagation, and durability are being considered, and methods for in-situ health monitoring are being developed. Though still in infancy, this program has already achieved significant results.

A set of experimental tests has been performed for the determination of the fracture toughness of the bond between a fiberglass/polyester composite-material overlay and a concrete substrate. To our knowledge, these tests are the first of their kind, and experimental methods and procedures had to be developed for both specimen fabrication and specimen testing. Methods and procedures were adapted from existing ASTM standards for the adhesion of metallic (ASTM D3433-93) and composite (ASTM D5528-94a) double cantilever beam (DCB) specimens. Specimen geometry and fabrication, loading devices and specimen support, and testing methods had to be developed *ab initio.*

The data collected during this experiment allowed the determination of the fracture properties of the bond between the erglass/polyester composite-material overlay and the concrete substrate. The strain energy release rate, G, was termined as a measure of the bond fracture toughness. Two sets of specimens were fabricated tested. The second set of specimens was fabricated after the results from the testing of the first set of specimens were analyzed. Thus, the second set of specimens benefited from the knowledge accumulated in the fabrication and testing of the first set. Not surprisingly,

the results from the testing of the second set of specimens are significantly better than the results from the first set. For the first set of specimens, the average values of the strain energy release rate (SERR) were of the order $G_{average}$ = 0.1 J/mm. For the second set of specimens, strain energy release rates of the order $G_{average}$ = 0.252 J/mm were found. Additionally, the results obtained for the first set of specimens presented much more scatter than those for the second set of specimens. In the first set of specimens, the observed SERR values varied extensively from a high of 0.265 J/mm (specimen D1) to a low of 0.059 J/mm (specimen D6). In the second set of specimens, the observed SERR values varied much less, from a high of 0.241 J/mm (specimen S4) to a low of 0.229 J/mm (specimen S5).

The tests also allowed us to examine the nature of crack propagation in the bond between fiberglass/polyester composite-material overlay and a concrete substrate. The specimens with high fracture toughness had a large proportion of crack propagation inside the concrete substrate, while the specimens with low fracture toughness had crack propagation predominantly in the interface. When cracks propagated inside the concrete substrate, the crack path was contained in the superficial concrete-paste layer, which is expected to present weaker fracture toughness than the bulk of the concrete. The specimens that had cracks propagating in the interface are believed to be deficient from the point of view of specimen fabrication. However, these results are nevertheless valuable, since they may be representative of real-life situation when insufficient attention is paid to the details of composite material handling and fabrication.

Future efforts in this direction should concentrate first on improving the specimen fabrication procedure with special emphasis on repeatability and quality control. Further tests should be performed with the same concrete and composite systems, until more consistent results are achieved. Subsequently, the method can be extended to the study of other composite and concrete systems. For example, other composite systems could include fiberglass/epoxy, carbon/epoxy, fiberglass-grid/epoxy, etc., while other concrete systems could be quick cure concrete; high performance concrete, etc. Further extension of the method would be to specimens that have been exposed to environmental attacks, such as water submersion, temperature-humidity cycles, and ultraviolet exposure.

7. ACKNOWLEDGMENTS

The authors gratefully acknowledge the financial support of the National Science Foundation through NSF/EPSCoR Cooperative Agreement No. EPS-9630167 and of the South Carolina Research Institute. The composite materials and the expert advice received from the Reichhold Chemicals Corporation were invaluable in making this effort at all happen.

8. REFERENCES

1. ACI Committee 440, "State-of-the-Art Report on FRP for Concrete Structures", ACI 440R-96, American Concrete Institute, Farmington Hills, Mich., 68 pp.
2. Arduini, M., D'Ambrisi, A., and Di Tommaso, A., "Shear Failure of Concrete Beams Reinforced with FRP Plates", Proceedings, New Materials and Methods for Repair, ASCE, San Diego, Nov. 13-16, 1994, pp. 415-423.
3. Arduini, M., Di Tommaso, A., and Nanni, A., "Brittle Failure in FRP Plate and Sheet Bonded Beams", ACI Structural Journal, V. 94, No. 4, July-Aug. 1997, pp. 363-370.
4. Arduini, M., Nanni, A., "Parametric Study of Beams with Externally Bonded FRP Reinforcement", ACI Structural Journal, V. 94, No. 5, Sept.-Oct. 1997, pp. 493-501.
5. ASTM D 3433-93, "Standard Method for Fracture Strength in Cleavage of Adhesives in Bonded Metal Joints", American Society for Testing and Materials, 100 Barr Harbor Dr., West Conshohocken, PA 19428-2959.
6. ASTM D 5041-93b, "Standard Method for Fracture Strength in Cleavage of Adhesives in Bonded Joints", American Society for Testing and Materials, 100 Barr Harbor Dr., West Conshohocken, PA 19428-2959.
7. ASTM D 5528-94a, "Standard Method for Mode I Interlaminar Fracture Toughness of Unidirectional Fiber-Reinforced Polymer Matrix Composites", American Society for Testing and Materials, 100 Barr Harbor Dr., West Conshohocken, PA 19428-2959.
8. Cao, H. C. and Evans, A. G., "An Experimental Study of the Fracture Resistance of Bimaterial Interfaces", *Mechanics of Materials*, Vol. 7, 1989, pp. 295-304.
9. Chajes, M.J., Thomson, T. A., Januszka, T.F., and Fin, W., "Flexural Strengthening of Concrete Beams Using Externally Bonded Composite Materials", Construction and Building Materials, 1994, Vol. 8, No. 3, pp. 191-201.
10. El-Badry, M. (editor), "Advanced Composite Materials in Bridges and Structures", Proceedings, ACMBS-II, Montreal, Canada, 1996, 1027 pp.
11. Giurgiutiu, V., Dillard A. D., Dillard, G. J., Gagliano, J., Parvatereddy, H., "Criteria for the Prediction of Crack Propagation in Adhesive Layers", *Proceedings of the 20th Annual Meeting of the Adhesion Society,* February 23-26, 1997, Hilton Head Island, S. C.
12. J.J. Dussek, "Strengthening of Bridge Beams and Similar Structures by Means of Epoxy-Resin-Bonded External Reinforcement", Transportation Research Record, 785, Transportation Research Board, 1980, pp. 21-24.

13. Meier, U., Deuring, M., Meier, H., and Schwegler, G., "Strengthening of Structures with Advanced Composites", Alternative Materials for the Reinforcement and Prestressing of Concrete, I. L. Clarke (Ed.), Blackie Academic and Professional Pub., London, 1993, pp. 153-171.
14. Meier, U., Winistörfer, A., "Retrofitting Through External Bonding of CFRP Sheets", 2nd International RILEM Symposium FRPRCS-2, Ghent, 1995, pp. 465-472.
15. Meier, V. and Kaiser H., "Advanced Composite Materials in Civil Engineering Structures", Proceedings of the ASCE Specialty Conference, ASCE, New York, 1991, pp. 224-232.
16. Nanni, A., "CFRP Strengthening", ACI, Concrete International, June 1997, pp. 19-23.
17. Nanni, A., "Concrete Repair with Externally Bonded FRP Reinforcement: Examples from Japan", Concrete International, V. 17, No. 6, June 1995, pp. 22-25.
18. Perdikaris, Phillp C., Petrou, Michael F., Wong, Aidong, "Fatigue Strength and Stiffness of Reinforced Concrete Bridge Decks", Final Report No. FHWA/OH-93/016.
19. Quattrone, R., Berman, J., and Kamphaus, J., "Upgrade and Monitoring of Unreinforced Masonry Structures using Fiber Reinforced Polymers", *Proceedings of the International Composites Expo ICE-98*, Nashville, TN, January 19-21, 1998 (in press).
20. Reddy, D.V., Gervois, G. B., and Carlsson, L. A., "Laminate Bonding for Concrete Repair and Retrofit", Proceedings, Materials for the New Millennium, ASCE, 1996, pp. 1579-1591.
21. Rostasy, F. S., "FRP: The European Perspective", Proceedings, First International Conference on Composites in Infrastructure, Tucson, Arizona, 1996.
22. Rostasy, F.S. Hankers, C., and Ranisch, E.H., "Strengthening of R/C and P/C Structures with Bonded FRP Plates", Proceedings, 1st ACMBS International Conference, Sherbrooke, Quebec, Canada, pp. 253-263.
23. Saadatmanesh, H., and Ehsani, M., "RC Beams Strengthened with GFRP Plates" Part I and Part II, Journal of Structural Engineering, ASCE, Vol. 117, No. 11, Nov. 1991, pp. 3417-3455.
24. Scalzi, J.B., "The Future of Polymer Composites", Proceedings, First International Conference on Composites in Infrastructure, Tucson, Arizona, 1996.
25. SCDOT, "Supplemental Specification", S.C. File No.'s 22.636, December 6, 1994, pp1-5, 8.
26. Seible, F. and Karbhari, V., "Advanced Composites for Civil Engineering Applications in the United States", Proceedings, First International Conference on Composites in Infrastructure, Tucson, Arizona, 1996,
27. Tada, H., Paris, P. C., and Irwin, G. R., *The Stress Analysis of Cracks Handbook*, Del Research Corporation, 1989.
28. Triantafillou, T., Deskovic, N., and Deuring, M., "Strengthening of Concrete Structures with Prestressed Fiber Reinforced Plastic Sheets", ACI Structural Journal, May-June 1992, pp. 235-244.
29. Yoshizawa, H., Myojo, T., Okoshi, M., Mizukoshi, M., and Kliger, H. S., "Effect of Sheet Bonding Condition on Concrete Members Having Externally Bonded Carbon Fiber Sheet", Proceedings, Materials for the New Millennium, ASCE, 1996, pp. 1608-1616.